A Battery-less Contact Lens Sensor Prototype with Enhanced Performance for Cattle Health Monitoring

Sanjeev Kumar*, Dinesh R. Gawade*, Roy B. V. B. Simorangkir†, Gholamhosein Moloudian*,
Marco Belcastro*, Pasqualino Torchia*, Andrea Federico*, John L. Buckley* and Brendan O'Flynn*
*Tyndall National Institute, University College Cork, Dyke Parade, T12R5CP, Cork, Ireland.
†Department of Engineering, Durham University, DH1 3LE Durham, U.K.
E-mail: sanjeev.kumar@tyndall.ie

***Abstract*—This paper presents a low-cost, non-invasive, and fully integrated smart NFC sensor tag for cattle health monitoring. The proposed sensor solution operates without a battery and has the potential to measure the body temperature and health status of cattle. This paper expands on previous work in this area by the authors and demonstrates significant performance improvements, including flexibility for sensor replacement, simplified programming interfaces, and an extended wireless range. Among the various electronic components on the proposed NFC sensor tag, the microcontroller is identified as the most power-consuming, constituting over 76% of the total power consumption. Therefore, voltage and frequency scaling for the microcontroller have been employed to minimize the overall DC power consumption of the sensor tag. Furthermore, with an NFC-enabled smartphone, the developed sensor prototype achieves a measured wireless range of approximately 12 mm. Future work will investigate the further optimization of the smart contact lens for in-vivo operation.**

***Index Terms*—Battery-less NFC sensor tag, smart contact lens for cattle, energy harvesting, cattle health monitoring.**

I. Introduction

The health and well-being of cattle are of paramount importance for both livestock welfare and the sustainability of dairy and food industries. Timely detection and monitoring of health issues in cattle are crucial for disease prevention [1]. The conventional method for cattle health monitoring primarily relies on farmers' familiarity with their livestock and, when necessary, the intervention of a veterinarian. This existing approach is not only time-consuming and expensive but also prone to human error. Examining biomarkers in cattle's lacrimal or tear fluids enables the extraction of health-related parameters such as body temperature and blood glucose levels [2]. In recent years, there has been a growing interest in utilizing 13.56 MHz near-field communication (NFC) technology for non-invasive and battery-less cattle health monitoring, particularly through wearable sensors [2]–[6]. Currently, NFC technology not only facilitates contactless payments but also enables the passive wireless measurement of various health-related parameters. Several NFC-based smart contact lens sensor tags for wireless health monitoring of humans have been reported in existing literature [7]–[13]. These contact lens-integrated non-invasive wireless monitoring systems for health-related parameters include body temperature [7], glucose level monitoring [8], cholesterol monitoring [9], facilitate corneal wound healing [10], wireless immune-sensing of cortisol [11], monitoring and therapy of chronic ocular surface inflammation [12], and gaze tracking [13], among others. However, there has been limited research conducted on the development of smart contact lenses for wireless health monitoring of cattle. NFC-enabled smart contact lens solutions for collecting data on cattle health-related physiological parameters are reported in [2], [6], [14]. NFC sensing technology for measuring biomarkers in the tear fluid of a cow's eye for health monitoring is described in [2]. The authors of [14] have presented a prototype of a battery-less NFC sensor transponder designed for monitoring cattle temperature. Nevertheless, current NFC-based contact lens solutions reported in the literature have limitations, including a limited wireless communication range and non-optimized DC power consumption for the sensor tag [2], [14].

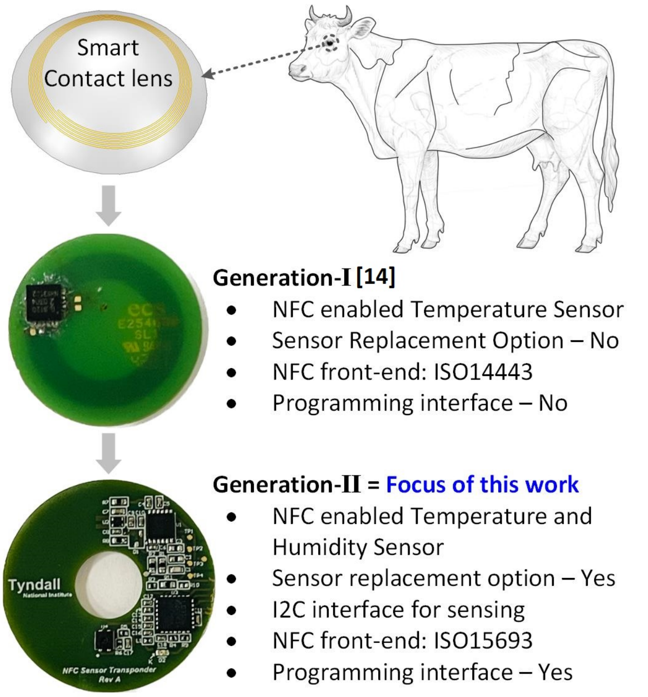

Fig. 1. Overview of the design evolution of NFC-enabled smart contact lens sensor tags for cattle health monitoring.

This paper presents a new NFC sensor tag with enhanced performance compared to the sensor tag previously reported by the authors in [14]. Fig. 1 illustrates the design evolution of NFC tags, with the proposed sensor denoted as Generation-II and the previously reported tag as Generation-I.

The Generation-I tag was shown to have limited capabilities, and the proposed tag aims to address these limitations. As depicted in Fig. 1, Generation-I had NFC-enabled temperature sensing capabilities but lacked the option for sensor replacement and an on-board programming interface. In contrast, the Generation-II tag showcases significant performance improvements across several crucial dimensions when compared to Generation-I. Specifically, Generation-II incorporates an NFC-enabled Temperature and Humidity Sensor, offers a valuable sensor replacement option, employs an I2C interface for sensing purposes, utilizes an advanced NFC radio that is compliant with the ISO15693 standard, and introduces an on-board user-friendly programming interface. Here, the term *valuable sensor replacement option* refers to the potential to replace the current Temperature and Relative Humidity Sensor (SHTC3) with custom-developed sensors such as a glucose sensor, without necessitating alterations to the hardware architecture. In addition, the DC power consumption of the microcontroller unit (MCU) has been optimized to minimize the overall power consumption of the Generation-II tag.

The aforementioned features of the proposed NFC sensor tag demonstrate significant performance enhancements, leading to improved functionality and versatility in cattle health monitoring. This paper is organized as follows: In Section II, the system architecture, hardware design, and prototype of the sensor tag are presented. In Section III, the measured results in terms of DC power consumption and wireless communication range of the tag are described. Finally, in Section IV, the paper is concluded, and the proposed future works are outlined.

II. Hardware Design and Prototype

A. System Architecture of the Proposed NFC Sensor Tag

Fig. 2 illustrates a block diagram of the proposed battery-less NFC sensor tag. The tag harvests radio-frequency (RF) energy from a reader, such as an NFC type 5 smartphone. An NFC-enabled smartphone comprises a coil antenna that energizes the NFC loop antenna in the tag through inductive coupling, subsequently enabling the NFC loop antenna to deliver RF power to the NFC radio. The internal rectifier and energy harvesting circuitry of the NFC radio perform RF to DC conversion. The DC output of the radio is denoted as the harvested voltage (V_{H}), which is regulated using a linear low dropout (LDO) voltage regulator, resulting in a stable 1.8 V DC output that supplies power to all the tag electronics. The proposed sensor tag utilizes the STM32L031G6U6 MCU [15] and the ST25DV16K-JFR6D3 NFC radio transceiver [16] from ST Microelectronics, SHTC3 Temperature (T) and Relative Humidity (RH) Sensor from Sensirion [17], and the TLV713 LDO voltage regulator [18] from Texas Instruments. Among various STM32 MCU options, the STM32L03 series was chosen primarily because these MCUs belong to STMicroelectronics' 32-bit ultra-low-power lineup, specifically designed for achieving low power consumption [15].

To achieve seamless digital communication between the MCU, radio transceiver, and sensor, the inter-integrated circuit (I2C) protocol is adopted. Furthermore, an on-board

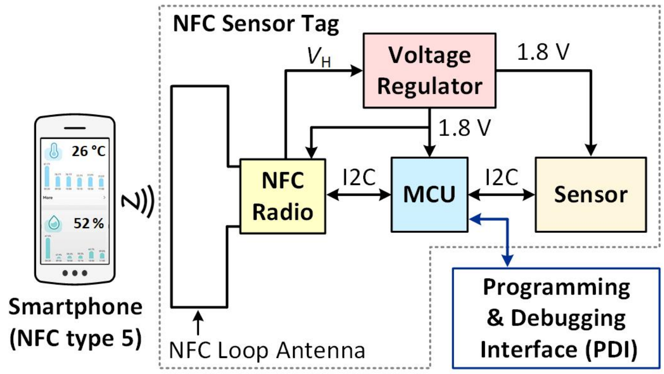

Fig. 2. Block diagram of the proposed NFC temperature and RH sensor tag.

programming and debugging interface (PDI) is provided for uploading firmware to the NFC sensor tag. When powered up, temperature (T) and relative humidity (RH) parameters are measured, and the MCU writes the measured sensor data to the integrated non-volatile memory (EEPROM) of the NFC radio transceiver. Subsequently, the NFC radio forwards the measured sensor data to an NFC type 5 smartphone in the form of an NFC data exchange format (NDEF) message using load modulation [19].

B. DC Power Consumption Estimation of the Tag

It is known that the strength of the magnetic field diminishes in proportion to the cube of the distance separating two mutually coupled coils, such as the coil within a smartphone and the NFC loop antenna of the sensor tag [20], [21]. Consequently, for a given separation between the smartphone and the sensor tag, there exists a limitation on the RF power available for harvesting by the NFC sensor. Therefore, there is a need to optimize the NFC sensor tag to operate with minimal DC power consumption. Fig. 3 depicts a pie chart that illustrates the distribution of maximum DC power consumption among the main components of the tag, namely the MCU, NFC radio, and sensor unit. The values represented in the pie chart are derived from the respective datasheets of the ICs [15]–[17]. It can be seen that the collective DC power consumption of the sensor and the NFC radio is less than 24% of the total power consumption of the tag (i.e., 12.69 mW). With a maximum DC power consumption of 9.72 mW, the MCU is identified as the most power-hungry component in the sensor tag, contributing to over 76% of the total power consumption of the tag.

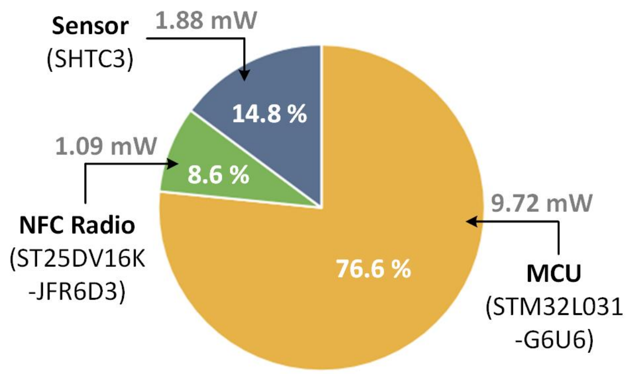

Fig. 3. DC Power consumption of various IC components of the tag.

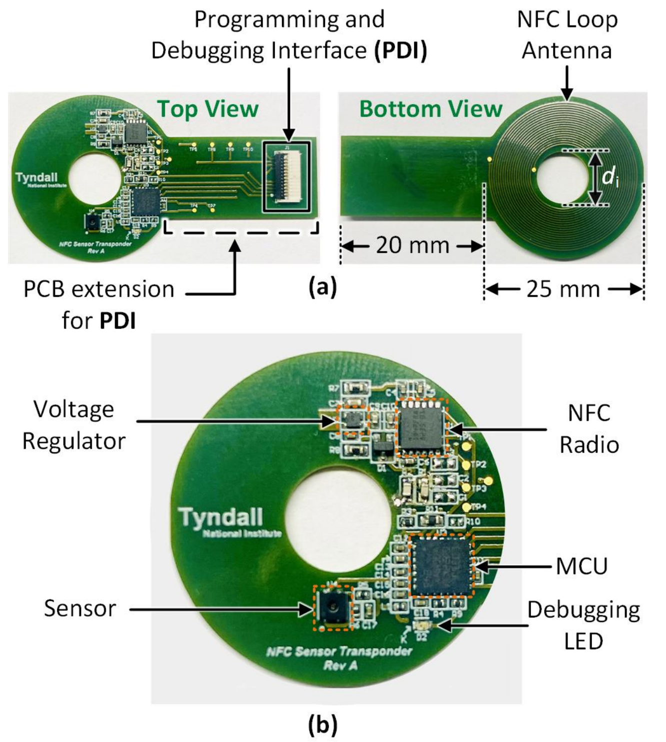

Fig. 4. Hardware prototype: (a) Top and bottom view of the NFC sensor with PCB extension for tag programming and debugging, (b) Top view of the proposed smart contact lens sensor tag when PDI extension is removed.

Hence, in this work, the power consumption of the MCU has been optimized to minimize the overall DC power consumption of the NFC sensor tag, as detailed in Section III-A.

C. Prototype of Proposed NFC Sensor Tag

The fabricated prototype of the proposed NFC sensor tag is illustrated in Fig. 4. The sensor tag was designed using an electronics printed circuit board (PCB) design platform, Altium Designer. The PCB is fabricated using a 4-layer PCB using a low-cost FR-4 substrate with a total thickness of 0.96 mm. All Surface Mount Device (SMD) components are populated on the top side of the PCB for ease of assembly, convenience in hardware testing and debugging, and cost-effectiveness. Fig. 4(a) depicts the top and bottom views of the sensor tag, which also includes a rectangular PCB extension to accommodate the programming and debugging interface (PDI). The NFC loop antenna is fabricated on the back side of the PCB using 35 μm thick copper. This loop antenna has a total of 19 turns with a trace width of 0.15 mm and a spacing of 0.2 mm between consecutive traces. The firmware is uploaded to the tag through the PDI interface, and once the firmware is uploaded, the rectangular PDI extension of the PCB is removed, resulting in the final proposed prototype, as shown in Fig. 4(b). The final prototype has an outer diameter of 25 mm and an inner diameter d_i = 8 mm. Fig. 4(b) also labels the essential SMD components, including the NFC radio, MCU, sensor, voltage regulator, and debugging LED.

TABLE I
MEASURED DC POWER CONSUMPTION OF THE SENSOR TAG WITH VARYING MCU VOLTAGE AND CLOCK FREQUENCY.

Design Iteration	MCU Clock Source	f_{CLK} (MHz)	V_{DD} (V)	V_{CORE} (V)	Measured DC Power Consumption (mW)
1	HSI	16	3.3	1.8	12.69
2	HSI	16	1.8	1.8	5.76
3	HSI	8	1.8	1.5	3.38
4	MSI	4.192	1.8	1.5	1.89
5	MSI	2.096	1.8	1.2	1.35
6	MSI	0.524	1.8	1.2	0.86
7	MSI	0.262	1.8	1.2	0.74

III. RESULT AND DISCUSSION

In this section, the techniques employed to minimize the DC power consumption of the developed NFC smart contact lens sensor tag are described. Additionally, the measured wireless communication range and the sensor parameters obtained from the developed NFC sensor tag have been presented. Finally, the performance enhancements achieved for the proposed tag (Generation-II) compared to the previous work (Generation-I) have been described.

A. Optimization of DC Power Consumption

The DC power consumption of CMOS ICs (e.g., MCUs) varies quadratically with the supply voltage and linearly with the MCU clock frequency, f_{CLK} [22]. Therefore, in this work, a combination of voltage and frequency scaling techniques has been employed to minimize the power consumption of the proposed sensor tag. The reduction in the measured DC power consumption of the sensor tag was accomplished through a total of 7 design iterations, as summarized in Table I. The measured DC power consumption of the tag is a function of the following key parameters of the MCU: clock source mode, clock frequency f_{CLK}, MCU voltage (V_{DD}), and core voltage (V_{CORE}). In the initial design iteration, a measured DC power consumption of 12.69 mW was recorded with clock source mode = high speed internal (HSI) RC oscillator, f_{CLK} = 16 MHz, V_{DD} = 3.3 V, and V_{CORE} = 1.8 V. In the second iteration, while keeping all other parameters constant and reducing the value of V_{DD} to 1.8 V, the DC power consumption of the tag dropped to 5.76 mW. Subsequent design iterations achieved further reductions in DC power consumption by changing the MCU clock source mode from HIS to MSI (multi-speed internal) and lowering both the clock frequency and core voltage of the MCU. For the final, seventh design iteration (clock source mode = MSI, f_{CLK} = 0.262 MHz, V_{DD} = 1.8 V, and V_{CORE} = 1.2 V), the measured DC power consumption of the NFC sensor tag was reduced to 0.738 mW, which is 17 times lower than the power consumption measured at the beginning i.e., in iteration 1 of the power consumption optimization process.

Table II presents a performance comparison of the developed NFC sensor tag with the state-of-the-art literature. The

TABLE II
COMPARISON OF WIRELESS TECHNOLOGY TECHNICAL PARAMETERS.

Ref.	MCU Clock (MHz)	Tag Coil Size (mm)	DC Power Consumption (mW)	Range (mm)
[23]	1	12×16	1.74	8
[24]	1	$\pi \times 13^2$	1.72	10
[25]	NA	35×25	1.8	10
[32]	NA	10×5	0.9	10
[26]	1	50×50	5.29	18
[27]	NA	43×58	4.45	19
[28]	1	50×50	3	20
[29]	1	50×50	5.29	20
[30]	1	50×50	8	19
[31]	NA	34×46	1.3	30
[33]	1	35×35	2.1	30
[3]	0.524	49×59	0.59	50
This Work	0.262	$\pi \times 12.5^2$	0.74	12

table reveals that the power consumption of the majority of NFC sensor tags in existing literature exceeds 1 mW [23]–[31], with only two tags achieving DC power consumption lower than 1 mW [3], [32]. It is evident from Table II that the NFC tag developed in this work has a peak DC power consumption of 0.738mW, marking it as one of the lowest values reported in existing literature. Additionally, Table II illustrates the wireless communication range of the NFC tags reported in the literature, showcasing that the sensor tag developed in this work demonstrates optimal range performance despite its considerably small coil size.

B. Measurement of Wireless Range and Sensor Parameters using a Smartphone

As shown in Fig. 5, an NFC Type 5 Samsung Galaxy A52 smartphone was employed for the purpose of testing and evaluating both the wireless communication range of the sensor prototype and the retrieval of sensor data from the developed NFC sensor tag. The prototype NFC sensor tag is powered by the smartphone, enabling the measurement of sensor data on the smartphone's display screen without the need for a battery. The measurements showed that the wireless communication range of the developed NFC sensor tag is approximately 12 mm.

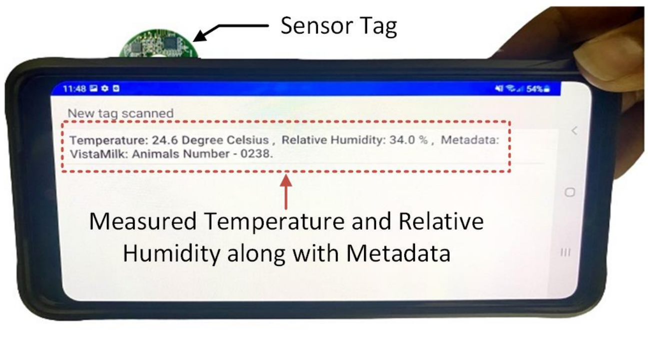

Fig. 5. Measurement of wireless range and T & RH sensor parameters using an NFC type 5 enabled smartphone (Samsung Galaxy A52).

TABLE III
PERFORMANCE COMPARISON: GENERATION-I VS GENERATION-II.

No.	Parameter	Generation I	Generation II
1	Programming Interface	No	Yes
2	Sensing Capability	Temperature	Temperature & Relative Humidity
3	Multi-sensor capability	No	Yes (using I2C)
4	NFC front-end	ISO14443	ISO15693
5	Interoperability	NFC Type 1, 2, 4	NFC Type 5
6	Memory (kB)	2	16
7	Wireless Range using a Phone	5 mm	12 mm

For the wireless acquisition of sensor data (including temperature and relative humidity) alongside supplementary metadata, the smartphone was positioned in close vicinity to the NFC sensor tag, at a distance of less than 12 mm. Fig. 5 visually shows the measured sensor data along with metadata (e.g., project name and animal number) on the smartphone's display.

C. Performance Enhancement Compared to Generation-I Tag

The key parameters distinguishing Generation-II from Generation-I NFC sensor tags are summarized in Table III. Generation-I tag does not have an on-board programming and debugging interface. On the other hand, Generation-II offers an easy programming and debugging experience with the inclusion of an on-board PDI interface. Furthermore, Generation-II enhances sensing capability by supporting both temperature (T) and relative humidity (RH) measurements. Additionally, Generation-II enhances the tag's adaptability by introducing the option of sensor replacement through the I2C interface. For example, the current SHTC3 sensor can easily be replaced with a compatible glucose sensor. Furthermore, to achieve performance improvements for Generation-II, the NFC front-end was upgraded from ISO14443 to ISO15693. Moreover, Generation-II is an NFC Type 5 tag and features eight times more memory compared to Generation-I. Furthermore, with an NFC Type 5-enabled smartphone, the Generation-II tag achieves a larger wireless range of 12 mm compared to approximately 5 mm for Generation-I.

IV. CONCLUSIONS AND FUTURE WORKS

This paper has presented a performance-enhanced battery-less smart contact lens sensor for future cattle health monitoring applications. The newly developed NFC sensor tag has exhibited significant performance improvements when compared to the previous generation tag. Key performance advancements encompass added flexibility for sensor replacement, simplified programming methods, and an extended read range. The experimental wireless read range achieved with a Samsung Galaxy A52 smartphone for the developed prototype of the sensor tag measures approximately 12 mm. In addition, voltage and frequency scaling techniques were strategically employed to minimize the DC power consumption of the microcontroller, yielding a peak consumption of 0.738 mW which is one of the lowest values reported in the literature. Future work will involve integrating a glucose sensor into the tag, as well as refining the current NFC sensing system to make it compatible with flexible, transparent, and biocompatible materials suitable for contact lens applications and in-vivo characterization.

Acknowledgment

This paper has emanated from research funding provided by Science Foundation Ireland (SFI) as part of the SFI Centre VistaMilk (SFI 16/RC/3835). Aspects of this work have been supported under the following Grant Numbers: CONNECT Centre (13/RC/2077), Insight Centre (SFI/12/RC/2289-2) and 16/RC/3918-CONFIRM, as well as the Enterprise Ireland funded Holistics DTIF (EI-DT20180291-A).

References

[1] B. Sharma and D. Koundal, "Cattle health monitoring system using wireless sensor network: a survey from innovation perspective," *IET Wireless Sensor Systems*, vol. 8, no. 4, pp. 143–151, 2018.

[2] M. Pigeon, N. Rather, B. O'Flynn, and J. Buckley, "NFC sensing of tear fluid for animal health monitoring," in *2021 15th European Conference on Antennas and Propagation (EuCAP)*, 2021, pp. 1–5.

[3] D. R. Gawade, S. Kumar, R. B. V. B. Simorangkir, B. O'Callaghan, D. Iacopino, N. Rather, B. O'Flynn, and J. L. Buckley, "Performance characterization of a battery-less NFC sensor for museum artifact monitoring," in *2023 34th Irish Signals and Systems Conference (ISSC)*, 2023, pp. 1–7.

[4] S. Kumar, J. Buckley, J. Barton, and B. O'Flynn, "Performance analysis of a novel flexible NFC tag for IoT applications," *12th Smart Systems Integration Conference*, pp. 432–435, 2018.

[5] D. R. Gawade, S. Ziemann, S. Kumar, D. Iacopino, M. Belcastro, D. Alfieri, K. Schuhmann, M. Anders, M. Pigeon, J. Barton, B. O'Flynn, and J. L. Buckley, "A smart archive box for museum artifact monitoring using battery-less temperature and humidity sensing," *Sensors*, vol. 21, no. 14, 2021.

[6] M. Zhang, X. Wang, H. Feng, Q. Huang, X. Xiao, and X. Zhang, "Wearable internet of things enabled precision livestock farming in smart farms: A review of technical solutions for precise perception, biocompatibility, and sustainability monitoring," *Journal of Cleaner Production*, vol. 312, 2021.

[7] M. Yuan, R. Das, E. McGlynn, R. Ghannam, Q. H. Abbasi, and H. Heidari, "Wireless communication and power harvesting in wearable contact lens sensors," *IEEE Sensors Journal*, vol. 21, no. 11, pp. 12 484–12 497, 2021.

[8] D. H. Keum, S.-K. Kim, J. Koo, G.-H. Lee, C. Jeon, J. W. Mok, B. H. Mun, K. J. Lee, E. Kamrani, C.-K. Joo *et al.*, "Wireless smart contact lens for diabetic diagnosis and therapy," *Science advances*, vol. 6, no. 17, p. eaba3252, 2020.

[9] H. Song, H. Shin, H. Seo, W. Park, B. J. Joo, J. Kim, J. Kim, H. K. Kim, J. Kim, and J.-U. Park, "Wireless non-invasive monitoring of cholesterol using a smart contact lens," *Advanced Science*, vol. 9, no. 28, p. 2203597, 2022.

[10] Q. Wu, C. Yang, W. Chen, K. Chen, H.-j. Chen, F. Liu, D. Liu, H. Lin, X. Xie, and W. Chen, "Wireless-powered electrical bandage contact lens for facilitating corneal wound healing," *Advanced Science*, vol. 9, no. 31, p. 2202506, 2022.

[11] M. Ku, J. Kim, J.-E. Won, W. Kang, Y.-G. Park, J. Park, J.-H. Lee, J. Cheon, H. H. Lee, and J.-U. Park, "Smart, soft contact lens for wireless immunosensing of cortisol," *Science advances*, vol. 6, no. 28, p. eabb2891, 2020.

[12] J. Jang, J. Kim, H. Shin, Y.-G. Park, B. J. Joo, H. Seo, J.-e. Won, D. W. Kim, C. Y. Lee, H. K. Kim *et al.*, "Smart contact lens and transparent heat patch for remote monitoring and therapy of chronic ocular surface inflammation using mobiles," *Science Advances*, vol. 7, no. 14, p. eabf7194, 2021.

[13] L. Massin, F. Seguin, V. Nourrit, E. Daniel, J.-L. de Bougrenet de la Tocnaye, and C. Lahuec, "Smart contact lens applied to gaze tracking," *IEEE Sensors Journal*, vol. 21, no. 1, pp. 455–463, 2021.

[14] D. R. Gawade, B. V. B. Roy Simorangkir, S. Kumar, M. Pigeon, M. Belcastro, N. Rather, J. L. Buckley, and B. O'Flynn, "A battery-less NFC sensor transponder for cattle health monitoring," in *2023 IEEE Applied Sensing Conference (APSCON)*, 2023, pp. 1–3.

[15] *STMicroelectronics: Datasheet for STM32L031x4 STM32L031x6 microcontroller*, Accessed on: August 30, 2023. [Online]. Available: https://www.st.com/resource/en/datasheet/stm32l031k6.pdf.

[16] *STMicroelectronics: Datasheet for ST25DV16K NFC radio transceiver*, Accessed on: August 30, 2023. [Online]. Available: https://www.st.com/resource/en/datasheet/st25dv04k.pdf.

[17] *Sensirion: Datasheet for SHTC3 Humidity and Temperature Sensor IC*, Accessed on: August 30, 2023. [Online]. Available: https://www.sensirion.com/products/catalog/SHTC3/.

[18] *Texas Instruments: Datasheet for TLV713-low-dropout voltage regulator*, Accessed on: August 30, 2023. [Online]. Available: https://www.ti.com/lit/ds/symlink/tlv713.pdf.

[19] S. M. Ali, T.-B. Nguyen, and W.-Y. Chung, "New directions for skincare monitoring: An NFC-based battery-free approach combined with deep learning techniques," *IEEE Access*, vol. 10, pp. 27 368–27 380, 2022.

[20] U. Azad, *Near-Field Based Communication and Electrical Systems*. University of California, Los Angeles, 2013.

[21] Z. Su, B. O'Callaghan, S. Kumar, B. O'Flynn, J. Barton, S. Bulja, J. L. Buckley *et al.*, "Frequency dependence of loop antenna h-field in free-space," in *The 19th RIA/URSI Research Colloquium on Radio Science and Communications*. Royal Irish Academy, RIA, 2022, pp. 1–3.

[22] P. Oppermann and B.-C. Renner, "Acoustic backscatter communication and power transfer for batteryless wireless sensors," *Sensors*, vol. 23, no. 7, 2023.

[23] M. Boada, A. Lazaro, R. Villarino, E. Gil-Dolcet, and D. Girbau, "Battery-less nfc bicycle tire pressure sensor based on a force-sensing resistor," *IEEE Access*, vol. 9, pp. 103 975–103 987, 2021.

[24] S. M. Ali, T.-B. Nguyen, and W.-Y. Chung, "New directions for skincare monitoring: An nfc-based battery-free approach combined with deep learning techniques," *IEEE Access*, vol. 10, pp. 27 368–27 380, 2022.

[25] B. M. G. Rosa, S. Anastasova-Ivanova, and G. Z. Yang, "Nfc-powered flexible chest patch for fast assessment of cardiac, hemodynamic, and endocrine parameters," *IEEE Transactions on Biomedical Circuits and Systems*, vol. 13, no. 6, pp. 1603–1614, 2019.

[26] M. Boada, A. Lazaro, R. Villarino, and D. Girbau, "Battery-less nfc sensor for ph monitoring," *IEEE Access*, vol. 7, pp. 33 226–33 239, 2019.

[27] P. Escobedo, M. Fernández-Ramos, N. López-Ruiz, O. Moyano-Rodríguez, A. Martínez-Olmos, I. Pérez de Vargas-Sansalvador, M. Carvajal, L. Capitán-Vallvey, and A. Palma, "Smart facemask for wireless CO_2 monitoring," *Nature Communications*, vol. 13, no. 1, p. 72, 2022.

[28] M. Boada, A. Lazaro, R. Villarino, and D. Girbau, "Battery-less soil moisture measurement system based on a nfc device with energy harvesting capability," *IEEE Sensors Journal*, vol. 18, no. 13, pp. 5541–5549, 2018.

[29] A. Lazaro, M. Boada, R. Villarino, and D. Girbau, "Color measurement and analysis of fruit with a battery-less nfc sensor," *Sensors*, vol. 19, no. 7, p. 1741, 2019.

[30] M. Boada, A. Lazaro, R. Villarino, and D. Girbau, "Nfc battery-less colour sensor and its applications," in *2020 Global Congress on Electrical Engineering (GC-ElecEng)*. IEEE, 2020, pp. 46–50.

[31] B. Vennemann, D. Obrist, and T. Rösgen, "A smartphone-enabled wireless and batteryless implantable blood flow sensor for remote monitoring of prosthetic heart valve function," *PLoS One*, vol. 15, no. 1, p. e0227372, 2020.

[32] B. M. Rosa, S. Anastasova, and G. Z. Yang, "Nfc-powered implantable device for on-body parameters monitoring with secure data exchange link to a medical blockchain type of network," *IEEE Transactions on Cybernetics*, 2021.

[33] X. Qian, Z. Li, Z. Meng, N. Gao, and Z. Zhang, "Flexible rfid tag for sensing the total minerals in drinking water via smartphone tapping," *IEEE Sensors Journal*, vol. 21, no. 21, pp. 24 749–24 758, 2021.